Available online at www.sciencedirect.com
SCIENCE DIRECT
Journal of Catalysis 228 (2004) 298–310
JOURNAL OF CATALYSIS
www.elsevier.com/locate/jcat

Dibenzothiophene hydrodesulfurization activity and surface sites of silica-supported MoP, Ni_2P, and Ni–Mo–P catalysts

Fuxia Sun, Weicheng Wu, Zili Wu, Jun Guo, Zhaobin Wei, Yongxing Yang, Zongxuan Jiang, Fuping Tian, Can Li *

State Key Laboratory of Catalysis, Dalian Institute of Chemical Physics, Chinese Academy of Sciences, PO Box 110, Dalian 116023, China

Received 7 May 2004; revised 29 August 2004; accepted 3 September 2004

Available online 22 October 2004

Abstract

Silica-supported binary and ternary phosphides, MoP/SiO_2, Ni_2P/SiO_2, and $Ni–Mo–P/SiO_2$ have been prepared and characterized by X-ray diffraction (XRD), BET surface area, CO chemisorption, transmission electron microscopy (TEM), and infrared spectroscopy (IR). The hydrodesulfurization (HDS) activities of dibenzothiophene (DBT) were measured and compared at 593 K and 3.0 MPa for MoP/SiO_2, Ni_2P/SiO_2, and $Ni–Mo–P/SiO_2$ catalysts with different Mo and Ni loadings. The activities of the phosphides follow the order $Ni_2P/SiO_2 > Ni–Mo–P/SiO_2 > MoP/SiO_2$. The Ni sites in the $Ni–Mo–P/SiO_2$ catalysts play a major role in the conversion of DBT, and the activity of the catalysts increases with increasing Ni content. This is different from sulfides, nitrides, and carbides, as no synergetic effect is observed between the phosphided Ni and the Mo atoms. The surface of these phosphide catalysts is partially sulfided forming a surface phosphosulfide phase, while the bulk structure of the phosphides is maintained in the HDS reactions.

Keywords: Hydrodesulfurization; Transition metal phosphides; MoP; Ni_2P; NiMoP; Dibenzothiophene; IR spectroscopy; CO adsorption

1. Introduction

Interest in the development of novel catalysts for hydrodesulfurization has been spurred by the need to meet stringent environmental regulations that have recently been enacted throughout the world [1,2]. Typical hydrodesulfurization catalysts are alumina-supported sulfides of molybdenum or tungsten with either nickel or cobalt "promoter" [3,4] and often contain phosphorus as a secondary promoter [5,6]. These conventional catalysts are active in converting thiophene and benzothiophenes, but not active enough to desulfurize the most refractory sulfur-containing polyaromatic compounds [7,8]. This has led to a worldwide search for better catalysts for hydrodesulfurization. Current approaches include the improvement of existing sulfide catalysts and the investigation of new compositions such as carbides, nitrides, materials containing noble metals, and zeolites [9–12]. Transition metal phosphides have recently been reported as a new class of high activity hydroprocessing catalysts that have substantial promise as next-generation catalysts. They are regarded as a group of stable, sulfur-resistant, metallic compounds that have exceptional hydroprocessing properties [2,13]. Several articles have recently appeared in the literature describing the HDS properties of metal phosphide catalysts [14–25].

In this paper, various binary transition metal phosphides, such as MoP/SiO_2 and Ni_2P/SiO_2, were prepared by temperature-programmed reduction. Nickel is an effective promoter in sulfided $Mo/\gamma\text{-}Al_2O_3$ catalysts for hydrodesulfurization. In order to determine whether Ni has a similar effect on phosphides as in sulfides in HDS reactions, the ternary phosphides, silica-supported nickel molybdenum phosphide ($Ni–Mo–P/SiO_2$) with various loadings of NiO and MoO_3, were also prepared. The DBT HDS activities

* Corresponding author. Fax: +86 411 4694447.
E-mail address: canli@dicp.ac.cn (C. Li).
URL: http://www.canli.dicp.ac.cn.

0021-9517/$ – see front matter
doi:10.1016/j.jcat.2004.09.002

were measured and compared for MoP/SiO_2, Ni_2P/SiO_2, and $Ni–Mo–P/SiO_2$ catalysts with various Ni and Mo contents. It is found that the Ni_2P/SiO_2 catalyst has the highest DBT conversion and no synergetic effect is observed between phosphided Ni and Mo for the $Ni–Mo–P/SiO_2$ catalysts.

In order to gain insight into the nature of the phosphide catalysts under HDS conditions, the surface sites of reduced and sulfided MoP/SiO_2, Ni_2P/SiO_2, and $Ni–Mo–P/SiO_2$ catalysts were studied by IR spectroscopy using CO as the probe molecule. The IR results indicate that the surface of these phosphide catalysts is partially sulfided while the structure of the phosphides is retained under HDS reaction conditions. The evolved surface sites show some differences from those of sulfided Mo or sulfided Ni. It also suggests that Ni species more easily expose at the surface of the NiMoP particles. Metallic Ni plays a promoter role in the sulfidation of Mo in the catalyst. The working Ni_2P/SiO_2 catalyst surface may be a nickel phosphosulfide (i.e., NiP_xS_y) phase. This unique surface constitution of NiP_xS_y is supposed to be responsible for the excellent HDS activity of the Ni_2P/SiO_2 catalyst. The reactivity and spectroscopic results suggest that phosphides, especially nickel phosphide, are potentially promising materials for hydrodesulfurization reactions.

2. Experimental

2.1. Catalyst preparation

The syntheses of bulk and silica-supported MoP and Ni_2P have been described in the literature [15,24]. The details for the synthesis of nickel molybdenum phosphides are given below.

2.1.1. Bulk NiMoP

An aqueous solution of $(NH_4)_6Mo_7O_{24}\bullet 4H_2O$ and $(NH_4)_2HPO_4$ (Mo/P = 1) was mixed with an aqueous solution of $Ni(NO_3)_2\bullet 6H_2O$ (Ni/Mo = 1); a few drops of nitric acid were added in order to dissolve the precipitate. After evaporation of the water, the obtained solid was calcined in air at 773 K for 4 h and subsequently reduced from room temperature (RT) to 573 K at a rate of 5 K/min and from 573 to 973 K at a rate of 1 K/min in flowing H_2 (300 ml/min). The sample was kept at 973 K for another 2 h, followed by cooling to RT under helium flow (30 ml/min), and then passivated at RT in a stream of 1% O_2/He (30 ml/min).

2.1.2. Ni–Mo–P/SiO2

$Ni–Mo–P/SiO_2$ catalysts were prepared with different MoO_3 and NiO loadings. When the loading of MoO_3 was 15 wt%, the loadings of NiO were 2.3, 4.7, 7.8, 9.3, and 15 wt%, respectively. When the loading of NiO was 15 wt%, the loadings of MoO_3 were 2.0, 5.0, 7.0, 10, and 15 wt%, respectively. The silica-supported catalysts were prepared as described above for unsupported NiMoP catalysts.

2.2. Characterization

The XRD patterns of the passivated sample were taken on a Regaku Rotaflex (Ru-200b) powder X-ray diffractometer with a Cu-Kα radiation ($\lambda = 1.5418$ Å). The morphology and the particle size of the samples were studied by transmission electron microscopy (TEM) in a JEM-2000EX operating at 100 kV. BET surface area and average pore diameter of the samples were determined at liquid nitrogen temperature on a Micrometritics ASAP-2000 system by nitrogen adsorption at 77 K with a static measurement mode. The chemisorption of CO was measured by a flow technique using a pulse (100 µl) of CO in a He stream (100 ml/min). Usually, 0.1 g of a passivated sample was loaded into a quartz reactor and pretreated in H_2 at 773 K for 2 h. After being cooled in He, a pulse of CO in a He carrier flowing was injected at 280 K through a sampling valve.

2.3. Catalytic activity

The catalytic activities were measured in a flowing fixed-bed reactor. The feedstock (0.5 wt% dibenzothiophene in decalin) was introduced by a liquid feedstock pump. The reactor was operated at 3.0 MPa, 593 K, a WHSV (weight hourly space velocity) of 12 h^{-1}, and a H_2 flow rate of 60 ml/min. Temperature was monitored by a movable thermocouple mounted axially along the length of the reactor. The passivated phosphide catalyst was reduced in the reactor in flowing H_2 from room temperature to 773 K in 0.7 h and kept at this temperature for 2 h before changing to reaction temperature. The HDS reaction was sampled every 1 h and was analyzed by a gas chromatograph equipped with a flame ionization detector and a 30-m-long capillary column (HP-1).

2.4. IR studies

Each of the passivated phosphide (MoP/SiO_2 (MoO_3, 15 wt%), Ni_2P/SiO_2 (NiO, 15 wt%), and $Ni–Mo–P/SiO_2$ (Ni/Mo = 0.3, 1.0, and 1.9, MoO_3, 15 wt%; NiO, 2.3, 7.8, and 15 wt%), respectively) samples and mechanical mixtures of MoP/SiO_2 (MoO_3, 15 wt%) and Ni_2P/SiO_2 (NiO, 15 wt%, Ni/Mo = 0.3, 1.0, and 1.9) were pressed into a self-supporting wafer (ca. 15 mg/cm^2) and put into a quartz IR cell with CaF_2 windows. The details of the IR experiments have already been published previously [25]. The catalyst sample was either reduced or sulfided in situ. The sample was reduced in flowing H_2 (200 ml/min) at 873 K for 2 h or pretreated with a mixture of thiophene/H_2 (10/100 Torr) at 593 K for 1 h or in a flow of 10 mol% H_2S/H_2 (60 ml/min) at 593 K for 1 h and then evacuated at 773 K for 20 min. As the sample was cooled down to RT, 15 Torr of CO was introduced into the IR cell.

All infrared spectra were collected on a Fourier transform infrared spectrometer (Nicolet Impact 410) with a resolution of 4 cm^{-1} and 64 scans in the region 4000–1000 cm^{-1}. All the spectra were obtained at RT in transmission mode after the sample was outgassed to high vacuum (10^{-5} Torr).

3. Results

3.1. XRD data

For supported MoP/SiO_2, Ni_2P/SiO_2, and $NiMoP/SiO_2$ samples, with MoO_3 and NiO loadings below 15 wt%, no XRD patterns of the MoP, Ni_2P, and NiMoP were discerned. Therefore, several phosphides with loading of 60 wt% MoO_3, 30 wt% NiO, 50 wt% NiMoP, and bulk phosphides were prepared for XRD references. Fig. 1 shows the XRD patterns of MoP and MoP/SiO_2, Ni_2P and Ni_2P/SiO_2, and NiMoP and $NiMoP/SiO_2$. The XRD patterns of bulk MoP, Ni_2P, and NiMoP (Fig. 1b, 1d, and 1f) are similar to the standard patterns from the powder diffraction file (PDF) [26] as well as that reported in the literature [15,24,27]. The diffraction patterns for MoP/SiO_2 with 60 wt% MoO_3 (Fig. 1a), Ni_2P/SiO_2 with 30 wt% NiO (Fig. 1c), and $NiMoP/SiO_2$ with 50 wt% NiMoP (Fig. 1e) exhibit peaks similar to those of bulk MoP, Ni_2P, and NiMoP, confirming that MoP, Ni_2P, and NiMoP crystallites are present on the silica support. The passivated MoP/SiO_2 (30 wt% MoO_3), Ni_2P/SiO_2 (15 wt% NiO), Ni–Mo–P/SiO_2 with 15 wt% MoO_3 and with loadings from 2.3 to 15 wt% NiO, or with 15 wt% NiO and loadings from 2.0 to 15 wt% MoO_3 samples only show the features of amorphous silica, indicating that the MoP, Ni_2P, and NiMoP particles on the SiO_2 support are too small to be detected by XRD when the MoO_3 and NiO loadings are low. It is possible that a pure NiMoP phase can be formed on the silica support with 15 wt% MoO_3 and 7.8 wt% NiO loadings, although no NiMoP crystallites can be observed on the support.

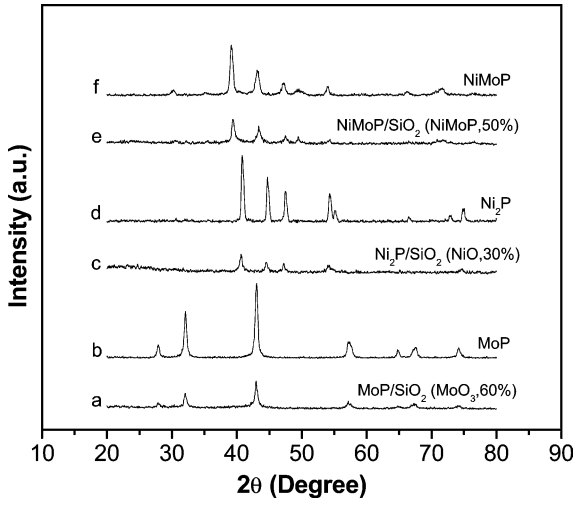

Fig. 1. X-ray diffraction patterns of (a) MoP/SiO_2 (MoO_3, 60 wt%); (b) bulk MoP; (c) Ni_2P/SiO_2 (NiO, 30 wt%); (d) bulk Ni_2P; (e) $NiMoP/SiO_2$ (NiMoP, 50 wt%); (f) bulk NiMoP.

3.2. TEM

Since no XRD patterns due to metal phosphides could be observed for the MoP/SiO_2 (MoO_3, 15 wt%), Ni_2P/SiO_2 (NiO, 15 wt%), $NiMoP/SiO_2$ (MoO_3, 15 wt%; NiO, 7.8 wt%), and Ni–Mo–P/SiO_2 (MoO_3, 15 wt%; NiO, 15 wt%) samples, TEM measurements were carried out on these samples and are presented in Fig. 2a, 2b, 2c, and 2d, respectively. Fig. 2 shows that MoP, Ni_2P, NiMoP, and Ni–Mo–P (Ni/Mo = 1.9) particles are homogeneously dispersed on the SiO_2 support and that the particle sizes of MoP, Ni_2P, NiMoP, and Ni–Mo–P (Ni/Mo = 1.9) are about 1–6, 1–10, 1–8, and 1–8 nm in diameter, respectively. The particles of Ni_2P show more agglomerated than those of MoP. The smaller particle size of Ni–Mo–P than of Ni_2P suggests that smaller particles are formed when Mo is present in the catalyst.

3.3. BET and pore texture

The BET surface areas (S_{BET}), average pore diameters, and Mo and Ni contents of the MoP/SiO_2, Ni_2P/SiO_2, and Ni–Mo–P/SiO_2 catalysts are given in Table 1. For Ni–Mo–P/SiO_2, when the loading of Mo was kept constant at a level corresponding to 15 wt% MoO_3, the loadings of NiO were 2.3, 4.7, 7.8, 9.3, and 15 wt%. For the sake of brevity, the catalysts with these loadings are denoted as M1, M2, M3 ($NiMoP/SiO_2$), M4, and M5, respectively. When the loading of Ni was kept constant at 15 wt% NiO, the Ni–Mo–P/SiO_2 catalysts with a content of MoO_3 at 2.0, 5.0, 7.0, and 10 wt% are abbreviated as M6, M7, M8, and M9, respectively (Table 1). The BET surface area of Ni_2P/SiO_2 is the lowest of all phosphides and that of MoP/SiO_2 is the highest (Table 1). The S_{BET} value of Ni–Mo–P/SiO_2 is between that of MoP/SiO_2 and Ni_2P/SiO_2. This suggests that the surface area is influenced by the different metal phosphide on the silica surface. The total pore volume (TPV) and pore diameter of Ni–Mo–P/SiO_2 have decreased compared to those of MoP/SiO_2 and Ni_2P/SiO_2.

3.4. CO chemisorption

The CO chemisorption capacities of the Ni–Mo–P/SiO_2 catalysts decrease with the increasing contents of Ni and the Ni_2P/SiO_2 catalyst exhibits the lowest value, 23.9 μmol CO/g (Table 2). This is consistent with the fact that Ni_2P on SiO_2 is more agglomerated, as revealed by the TEM.

3.5. Reactivity studies

A model fuel containing 0.5 wt% DBT in decalin was used to test the HDS activity for the MoP/SiO_2, Ni_2P/SiO_2, and Ni–Mo–P/SiO_2 catalysts. The conversions of DBT as a

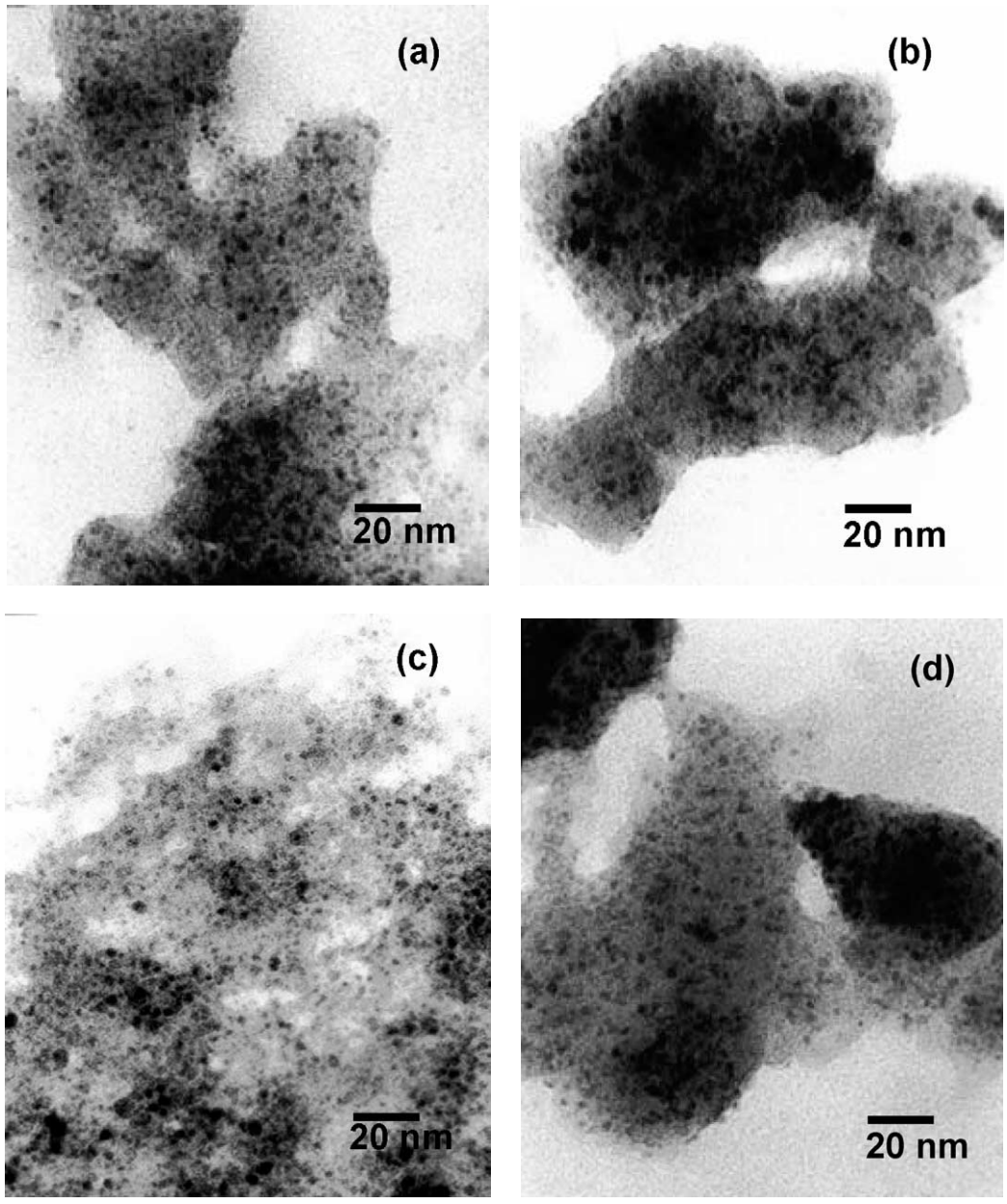

Fig. 2. TEM images of phosphide catalysts supported on silica. (a) MoP/SiO_2 (MoO_3, 15 wt%); (b) Ni_2P/SiO_2 (NiO, 15 wt%); (c) $NiMoP/SiO_2$ (MoO_3, 15 wt%; NiO, 7.8 wt%); (d) $Ni–Mo–P/SiO_2$ (MoO_3, 15 wt%; NiO, 15 wt%).

Table 1
BET surface area, total pore volume (TPV) and average pore diameters of silica-supported MoP, Ni_2P, and Ni–Mo–P catalysts

Catalyst	MoO_3 (%)	NiO (%)	BET (m^2/g)	TPV (cm^3/g)	Pore diameter (nm)	Abbreviation
MoP/SiO_2	15	–	303.8	0.70	9.2	
$NiMoP/SiO_2$	15	2.3	292.3	0.58	7.2	M1
$NiMoP/SiO_2$	15	4.7	281.9	0.55	7.2	M2
$NiMoP/SiO_2$	15	7.8	279.3	0.53	7.2	M3
$NiMoP/SiO_2$	15	9.3	271.8	0.54	7.2	M4
$NiMoP/SiO_2$	15	15	224.3	0.33	6.2	M5
$NiMoP/SiO_2$	2.0	15	227.0	0.41	7.2	M6
$NiMoP/SiO_2$	5.0	15	226.3	0.35	6.2	M7
$NiMoP/SiO_2$	7.0	15	226.2	0.32	5.7	M8
$NiMoP/SiO_2$	10	15	223.2	0.38	6.8	M9
Ni_2P/SiO_2	–	15	209.0	0.48	9.2	
SiO_2	–	–	467.2	0.99	8.5	

Table 2
CO chemisorption capacities of silica-supported MoP, Ni_2P, and Ni–Mo–P catalysts and DBT HDS activities after 6 h on stream

Catalyst	MoO_3 (%)	NiO (%)	Chemisorption capacity (μmol CO/g)	Areal rate (nmol DBT/(g_{cat} s))	TOF* ($\times 10^{-3}$ s^{-1})
MoP/SiO_2	15	–	135.3	8.3	0.1
$NiMoP/SiO_2$	15	2.3	134.6	16.0	0.1
$NiMoP/SiO_2$	15	4.7	112.2	17.8	0.2
$NiMoP/SiO_2$	15	7.8	94.4	28.1	0.3
$NiMoP/SiO_2$	15	9.3	41.9	33.0	0.8
$NiMoP/SiO_2$	15	15	29.9	40.5	1.4
Ni_2P/SiO_2	–	15	23.9	72.7	3.0

* Stoichiometry of CO/active site is assumed to be 1 for all samples.

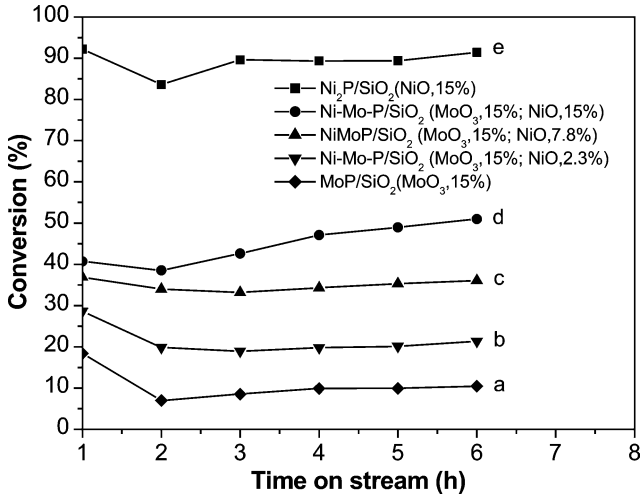

Fig. 3. Conversions of DBT HDS as a function of time on stream over (a) MoP/SiO_2 (MoO_3, 15 wt%); (b) Ni–Mo–P/SiO_2 (MoO_3, 15 wt%; NiO, 2.3 wt%); (c) $NiMoP/SiO_2$ (MoO_3, 15 wt%; NiO, 7.8 wt%); (d) Ni–Mo–P/SiO_2 (MoO_3, 15 wt%; NiO, 15 wt%); and (e) Ni_2P/SiO_2 (NiO, 15 wt%) catalysts, at 593 K, 3.0 MPa, and WHSV = 12 h^{-1}.

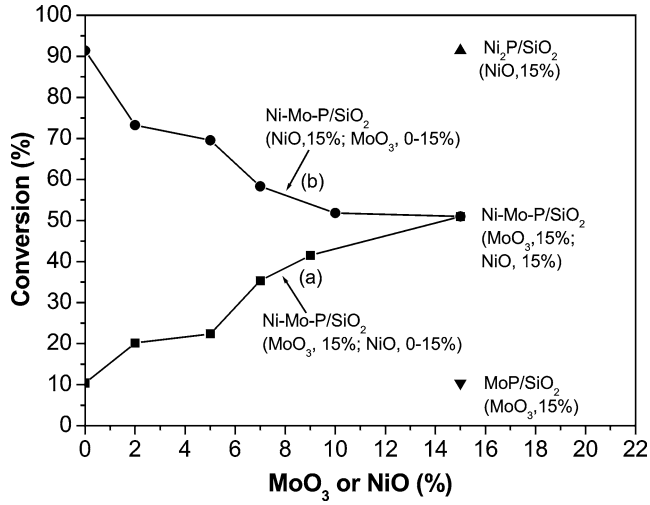

Fig. 4. HDS activities of dibenzothiophene after 6 h on stream for MoP/SiO_2 (MoO_3, 15 wt%); Ni_2P/SiO_2 (NiO, 15 wt%); (a) Ni–Mo–P/SiO_2 (MoO_3, 15 wt%; NiO, 2.3, 4.7, 7.8, 9.3, and 15 wt%, respectively); and (b) Ni–Mo–P/SiO_2 (NiO, 15 wt%; MoO_3, 2.0, 5.0, 7.0, 10, and 15 wt%, respectively) catalysts, at 593 K, 3.0 MPa, and WHSV = 12 h^{-1}.

function of time on stream over MoP/SiO_2 (MoO_3, 15 wt%), Ni_2P/SiO_2 (NiO, 15 wt%), and Ni–Mo–P/SiO_2 (MoO_3, 15 wt%; NiO, 2.3, 7.8, and 15 wt%) are shown in Fig. 3. The HDS activities increase with time, following an initial decline after the catalysts are brought on stream. For the $NiMoP/SiO_2$ catalyst, the conversion of DBT is between those of MoP/SiO_2 and Ni_2P/SiO_2 catalysts (Fig. 3a, 3c, and 3e). Fig. 4 presents the effect of Ni content on the HDS activities of Ni–Mo–P/SiO_2 with different loadings of MoO_3 and NiO after 6 h on stream. Ni_2P/SiO_2 shows the highest conversion of DBT (91%) and MoP/SiO_2 the lowest (10%). For the Ni–Mo–P/SiO_2 catalysts, the conversion of DBT increases with increasing Ni contents and their conversions are between 10 and 91% (see line a).

The DBT HDS activities after 6 h on stream are also presented in terms of areal rates and turnover frequencies (TOFs) in Table 2. The TOFs were calculated using the CO chemisorption capacities of reduced MoP/SiO_2, Ni_2P/SiO_2, and Ni–Mo–P/SiO_2 catalysts as a measurement of the number of active sites. The stoichiometry of a CO/active site is assumed to be 1. The TOF value of Ni_2P/SiO_2 is substantially higher than that of MoP/SiO_2, indicating that Ni_2P/SiO_2 is intrinsically more active than MoP/SiO_2.

The DBT HDS product distributions of the MoP/SiO_2, Ni_2P/SiO_2, and Ni–Mo–P/SiO_2 (including M1, M2, M3, M4, and M5) catalysts are shown in Fig. 5. The main products are biphenyl (BP), cyclohexylbenzene (CHB), and tetrahydrodibenzothiophene (H4-DBT). The BP selectivity of these phosphides is over 70%, much higher than that of CHB and H4-DBT, and MoP/SiO_2 shows the highest BP selectivity (84%). The BP selectivity of the Ni–Mo–P/SiO_2 catalysts is similar to that of MoP/SiO_2 when the NiO loadings are within 2.3–15 wt%. Ni_2P/SiO_2 also shows a high BP selectivity (79%). The selectivity of CHB for these phosphide catalysts is less than 26% and that of H4-DBT is less than 10%.

In order to further understand the nature of Ni–Mo–P/SiO_2 in the HDS reaction, the role of Mo in the Ni–Mo–P/SiO_2 catalyst was also investigated. The HDS reaction was tested for the catalysts with fixed Ni content (NiO, 15 wt%) and with different Mo loadings (MoO_3, 2.0, 5.0, 7.0, 10, and 15 wt%), i.e., the M6, M7, M8, M9, and M5 catalysts, respectively. The effect of Mo loading on the activities and the product distributions for these catalysts are presented in Figs. 4 and 6, respectively. Fig. 4 shows that the DBT conversion decreases with Mo addition and that Ni_2P/SiO_2

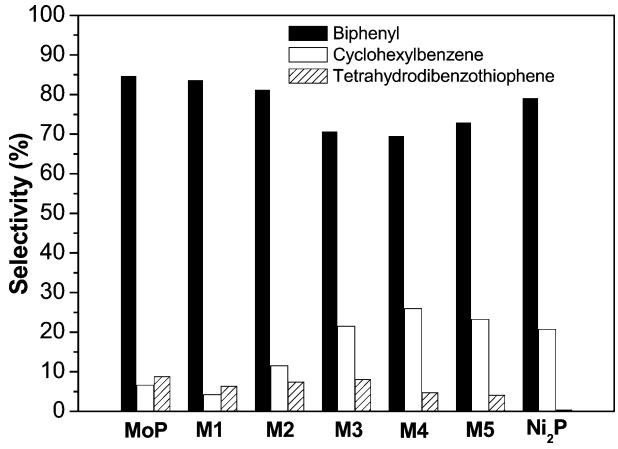

Fig. 5. Product distributions of DBT HDS after 6 h on stream for MoP/SiO_2 (MoO_3, 15 wt%), Ni_2P/SiO_2 (NiO, 15 wt%), and Ni–Mo–P/SiO_2 (MoO_3, 15 wt%; NiO, 2.3 wt% (M1); 4.7 wt% (M2); 7.8 wt% (M3); 9.3 wt% (M4), and 15 wt% (M5)) catalysts. The products are biphenyl (BP), cyclohexylbenzene (CHB), and tetrahydrodibenzothiophene (H4-DBT), at 593 K, 3.0 MPa, and WHSV = 12 h^{-1}.

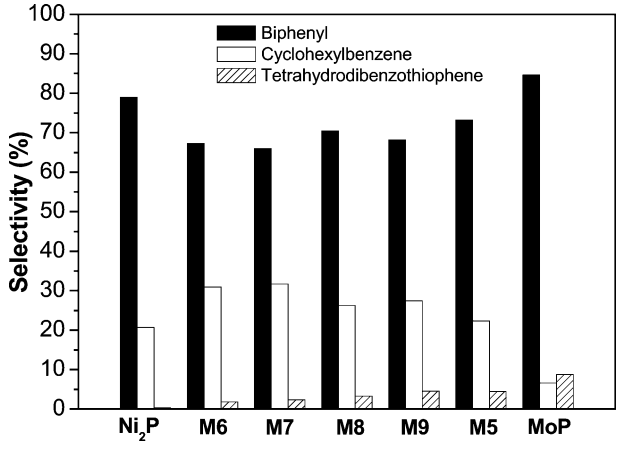

Fig. 6. Product distributions of DBT HDS after 6 h on stream for MoP/SiO_2 (MoO_3, 15 wt%), Ni_2P/SiO_2 (NiO, 15 wt%), and Ni–Mo–P/SiO_2 (NiO, 15 wt%; MoO_3, 2.0 wt% (M6); 5.0 wt% (M7); 7.0 wt% (M8); 10 wt% (M9), and 15 wt% (M5)) catalysts. The products are biphenyl (BP), cyclohexylbenzene (CHB), and tetrahydrodibenzothiophene (H4-DBT), at 593 K, 3.0 MPa, and WHSV = 12 h^{-1}.

(without MoO_3) is the most active catalyst for the DBT HDS reaction among all the phosphide catalysts (see line b). Thus, the comparison shows that the intrinsic activity of Ni_2P/SiO_2 is very high. For the Ni–Mo–P/SiO_2 catalysts (M6, M7, M8, M9, M5), the HDS activity is between those of MoP/SiO_2 and Ni_2P/SiO_2, similar to that of the Ni–Mo–P/SiO_2 catalysts (M1, M2, M3, M4, and M5). Fig. 6 also shows that MoP/SiO_2 and Ni_2P/SiO_2 have higher BP selectivity than Ni–Mo–P/SiO_2 catalysts. BP is the main product, the CHB selectivity is less than 35%, and the H4-DBT selectivity is below 10%.

For comparison, the catalytic activities of mechanically mixed samples of MoP/SiO_2 (MoO_3, 15 wt%) and Ni_2P/SiO_2 (NiO, 15 wt%) with different weight ratios (1/4, 2/3, 3/2, 4/1) were examined as well. The mixtures were prepared as follows: the MoP/SiO_2 (40/60 mesh) and Ni_2P/SiO_2 (40/60 mesh) were put into *n*-heptane; then the suspension was stirred and the mechanically mixed sample was obtained as the heptane evaporated. This procedure avoids possible phase contaminations between the compounds. The reaction results are presented in Table 3. They show that the DBT conversion decreases with decreasing weight ratio of Ni_2P/MoP. This indicates that the very high HDS activity of Ni_2P/SiO_2 plays the main role in the mixed catalysts. A similar catalytic performance was observed for the Ni–Mo–P/SiO_2 and mechanical mixture (MoP/SiO_2 + Ni_2P/SiO_2) catalysts with the variation of NiO/(NiO + MoO_3) molar ratio. All these phosphide catalysts show increased HDS activity with increased Ni contents.

Table 3
The conversions and selectivities in the HDS of DBT on MoP/SiO_2 (MoO_3, 15 wt%) (A) and Ni_2P/SiO_2 (NiO, 15 wt%) (B) catalysts and their mechanical mixtures

Catalyst	Conversion (%)	Selectivity (%)		
		BP*	CHB*	H4-DBT*
0.5 (g) (A)	10	84	7	9
0.5 (g) (B)	91	79	20.7	0.3
0.1 (g) A + 0.4 (g) B	58	84	14	2
0.2 (g) A + 0.3 (g) B	55	84	14	2
0.3 (g) A + 0.2 (g) B	33	84	11	5
0.4 (g) A + 0.1 (g) B	22	84	8	8

* BP (biphenyl), CHB (cyclohexylbenzene), H4-DBT (tetrahydrodibenzothiophene).

3.6. IR spectra of adsorbed CO

3.6.1. CO adsorption on reduced MoP/SiO_2, Ni_2P/SiO_2, and Ni–Mo–P/SiO_2 catalysts

As the freshly prepared phosphides will be oxidized when exposed to air, a passivation process is needed in order to avoid oxidation of the catalysts. As a consequence, a passivation layer is present on the passivated sample and investigation of the catalytic surface sites is only possible when this passivation layer is removed. Fig. 7 shows the IR spectra of CO adsorbed on passivated MoP/SiO_2, Ni_2P/SiO_2, and Ni–Mo–P/SiO_2 samples reduced by H_2 at 873 K. A characteristic IR band at 2042 cm^{-1} is detected for the reduced MoP/SiO_2 sample (Fig. 7a), which is nearly identical to the main band at 2045 cm^{-1} obtained for reduced MoP/SiO_2 before [25]. Therefore, this band can be assigned to linearly bonded CO on the Mo sites [10,28–32] on the surface of reduced MoP/SiO_2.

Three characteristic IR bands at 2082, 2056, and 1912 cm^{-1} are observed for CO adsorbed on reduced Ni_2P/SiO_2 (Fig. 7e), similar to those reported recently by Layman and Bussell [33]. CO is well suited for the characterization of nickel species on supported catalysts. The assignment of IR bands of adsorbed CO on nickel species supported and unsupported has been reported earlier [34–36]. The characteristic band at 2082 cm^{-1} can be attributed to terminally

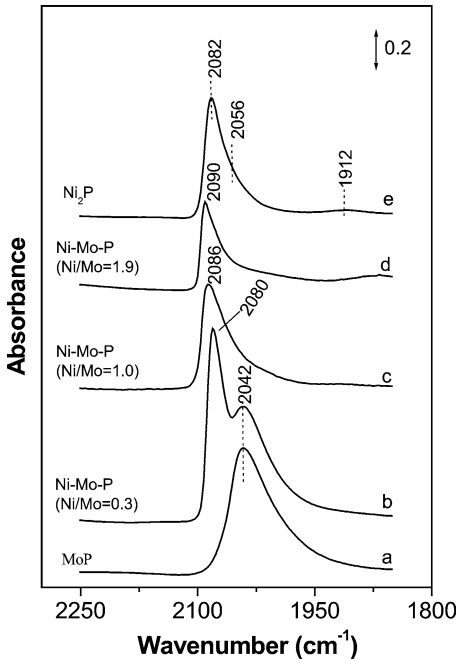

Fig. 7. IR spectra of CO adsorbed at room temperature on passivated phosphide catalysts reduced at 873 K for 2 h. (a) MoP/SiO_2 (MoO_3, 15 wt%); (b) $Ni–Mo–P/SiO_2$ (MoO_3, 15 wt%; NiO, 2.3 wt%), Ni/Mo = 0.3; (c) $NiMoP/SiO_2$ (MoO_3, 15 wt%; NiO, 7.8 wt%), Ni/Mo = 1.0; (d) $Ni–Mo–P/SiO_2$ (MoO_3, 15 wt%; NiO, 15 wt%), Ni/Mo = 1.9; (e) Ni_2P/SiO_2 (NiO, 15 wt%).

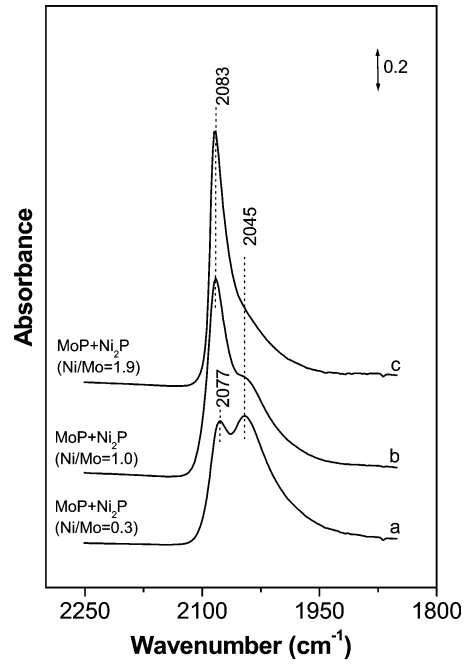

Fig. 8. IR spectra of CO adsorbed at room temperature on mechanically mixed MoP/SiO_2 (MoO_3, 15 wt%) and Ni_2P/SiO_2 (NiO, 15 wt%) samples reduced at 873 K for 2 h. (a) Ni/Mo = 0.3; (b) Ni/Mo = 1.0; (c) Ni/Mo = 1.9.

bonded CO on Ni sites on the surface of reduced Ni_2P/SiO_2. A shoulder at 2056 cm^{-1} can be due to a vibration of adsorbed $Ni(CO)_4$. The weak CO absorbance at 1912 cm^{-1} is assigned to CO adsorbed on Ni bridge sites on the surface of reduced Ni_2P/SiO_2.

The IR spectra of CO adsorbed on reduced $Ni–Mo–P/SiO_2$ samples with 15 wt% MoO_3 and different NiO contents of 2.3, 7.8, and 15 wt%, corresponding to Ni/Mo molar ratios of 0.3, 1.0, and 1.9, are presented in Fig. 7b, 7c, and 7d, respectively. Two IR bands at 2080 and 2042 cm^{-1} can be distinguished for the reduced $Ni–Mo–P/SiO_2$ sample with a Ni/Mo molar ratio of 0.3 (Fig. 7b). An IR band at 2086 cm^{-1} is observed for reduced $Ni–Mo–P/SiO_2$ with a Ni/Mo molar ratio of 1.0 (i.e., $NiMoP/SiO_2$) (Fig. 7c) and this band shifts to 2090 cm^{-1} for a Ni/Mo molar ratio of 1.9 (Fig. 7d). Combined with the IR spectra of reduced MoP/SiO_2 and reduced Ni_2P/SiO_2, the three IR bands at 2080, 2086, and 2090 cm^{-1} should be due to CO adsorbed on Ni sites and the band at 2042 cm^{-1} to CO adsorbed on Mo sites on the surface of reduced $Ni–Mo–P/SiO_2$. These results indicate that the catalyst surface is mainly dominated by Ni sites when the Ni/Mo molar ratio is one or larger; only when the loading of Ni is substantially lower than that of Mo, Mo sites appear on the surface of $Ni–Mo–P/SiO_2$.

To facilitate comparison with $Ni–Mo–P/SiO_2$ catalyst, IR spectra for CO adsorbed on reduced mechanically mixed samples of MoP/SiO_2 (MoO_3, 15 wt%) and Ni_2P/SiO_2 (NiO, 15 wt%) with different Ni/Mo molar ratios (Ni/Mo = 0.3, 1.0, and 1.9) were obtained and these are shown in Fig. 8a, 8b, and 8c, respectively. Two IR bands at 2077 and 2045 cm^{-1} can be distinguished for the mechanically mixed sample with a Ni/Mo molar ratio of 0.3 (Fig. 8a). An IR band at 2083 cm^{-1} and a shoulder at 2045 cm^{-1} are observed for the mechanically mixed sample with a Ni/Mo molar ratio of 1.0 (Fig. 8b), and a characteristic band at 2083 cm^{-1} is observed for the sample with a Ni/Mo molar ratio of 1.9 (Fig. 8c). The bands at 2083 and 2077 cm^{-1} can be attributed to CO adsorbed on Ni sites and the band at 2045 cm^{-1} to CO adsorbed on Mo sites on the surface of reduced mechanically mixed MoP/SiO_2 and Ni_2P/SiO_2 catalysts. These peak positions and intensities are similar to those of reduced $Ni–Mo–P/SiO_2$ catalysts shown in Fig. 7.

3.6.2. CO adsorption on MoP/SiO_2, Ni_2P/SiO_2, and $Ni–Mo–P/SiO_2$ pretreated with thiophene/H_2 and H_2S/H_2

Since phosphide catalysts exhibit a unique catalytic behavior in HDS reactions as shown by the above results and the literature [13,22,25], it is desirable to gain information on the surface properties of the working catalysts. IR spectroscopy combined with CO as probe molecule is a suitable technique for this goal. Thiophene/H_2 and H_2S/H_2 were selected to study their influences on the surface property of phosphide catalysts under conditions similar to those used in HDS reactions. Fig. 9 exhibits the IR spectra of CO adsorbed on MoP/SiO_2, Ni_2P/SiO_2, and $Ni–Mo–P/SiO_2$ pretreated with a thiophene/H_2 (10/100 Torr) mixture at 593 K for 1 h, which is the same temperature as in the DBT HDS reactivity tests. The characteristic band at 2042 cm^{-1} for the reduced

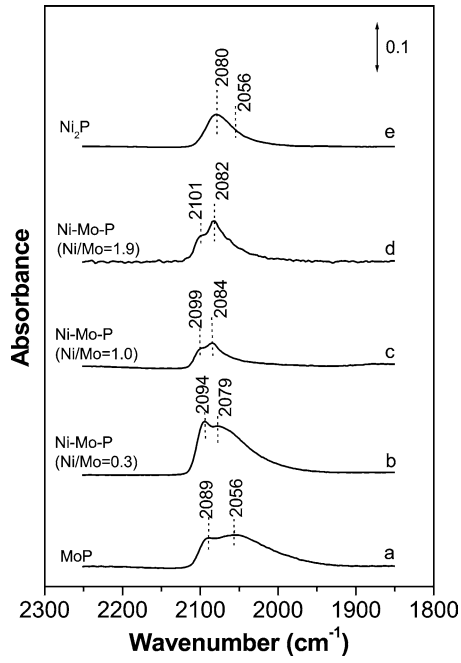

Fig. 9. IR spectra of CO adsorbed at room temperature on phosphide catalysts pretreated with a thiophene/H_2 (10/100 Torr) mixture at 593 K for 1 h. (a) MoP/SiO_2 (MoO_3, 15 wt%); (b) Ni–Mo–P/SiO_2 (MoO_3, 15 wt%; NiO, 2.3 wt%), Ni/Mo = 0.3; (c) NiMoP/SiO_2 (MoO_3, 15 wt%; NiO, 7.8 wt%), Ni/Mo = 1.0; (d) Ni–Mo–P/SiO_2 (MoO_3, 15 wt%; NiO, 15 wt%), Ni/Mo = 1.9; (e) Ni_2P/SiO_2 (NiO, 15 wt%).

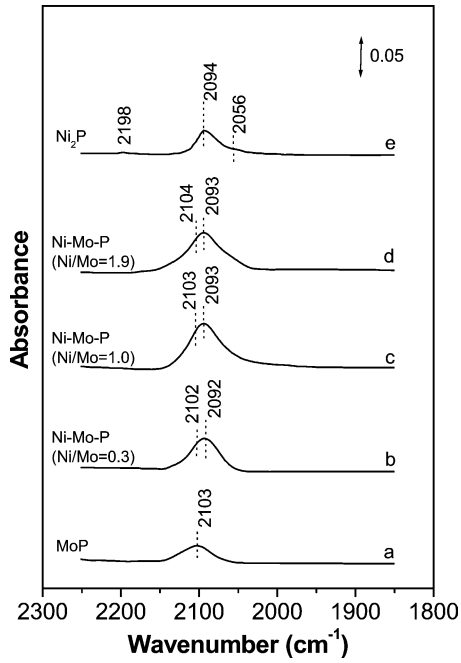

Fig. 10. IR spectra of CO adsorbed at room temperature on phosphide catalysts pretreated with a 10 mol% H_2S/H_2 mixture at 593 K for 1 h. (a) MoP/SiO_2 (MoO_3, 15 wt%); (b) Ni–Mo–P/SiO_2 (MoO_3, 15 wt%; NiO, 2.3 wt%), Ni/Mo = 0.3; (c) NiMoP/SiO_2 (MoO_3, 15 wt%; NiO, 7.8 wt%), Ni/Mo = 1.0; (d) Ni–Mo–P/SiO_2 (MoO_3, 15 wt%; NiO, 15 wt%), Ni/Mo = 1.9; (e) Ni_2P/SiO_2 (NiO, 15 wt%).

MoP/SiO_2 sample shifts to 2056 cm^{-1} for MoP/SiO_2 pretreated with thiophene/H_2. This shift is due to an increase in the dipole coupling between neighboring CO molecules due to fewer reduced Mo sites for CO adsorption. A new band at 2089 cm^{-1} appears which can be assigned to CO adsorbed on sulfided Mo sites (Fig. 9a). It suggests that the surface of the MoP/SiO_2 catalyst has been partially sulfided [25].

The characteristic band at 2082 cm^{-1} for the reduced Ni_2P/SiO_2 sample shifts to a lower wavenumber at 2080 cm^{-1} with a decrease in intensity when the Ni_2P/SiO_2 catalyst is treated with a mixture of thiophene/H_2 at 593 K for 1 h (Fig. 9e). It is possible that Ni_2P/SiO_2 is not sulfided under this sulfidation condition [33].

Two characteristic bands are obtained for Ni–Mo–P/SiO_2 samples with different Ni/Mo molar ratios after treatment with a mixture of thiophene/H_2, i.e., 2094 and 2079 cm^{-1} for a Ni/Mo molar ratio of 0.3 (Fig. 9b), 2099 and 2084 cm^{-1} for a Ni/Mo molar ratio of 1.0 (Fig. 9c), and 2101 and 2082 cm^{-1} for a Ni/Mo molar ratio of 1.9 (Fig. 9d). The IR bands at higher frequencies (2094, 2099, and 2101 cm^{-1}) can be due to CO adsorbed on sulfided Mo sites and the bands at 2079, 2084, and 2082 cm^{-1} can be ascribed to CO adsorbed on Ni sites on the surface of sulfided Ni–Mo–P/SiO_2 samples [25,34]. In addition, the asymmetry of the CO absorbance feature for Ni_2P/SiO_2 and Ni–Mo–P/SiO_2 catalysts suggests a small amount of $Ni(CO)_4$ formation for which an absorbance is observed at 2056 cm^{-1}.

Since Ni_2P/SiO_2 was not easily sulfided by the mixture of thiophene/H_2, as revealed by Fig. 9, more severe sulfiding conditions were employed in order to find out how resistant nickel phosphide is to sulfur treatment and to investigate CO adsorption on the sulfided Ni sites in phosphides. These phosphides were subjected to a flowing 10 mol% H_2S/H_2 mixture at 593 K for 1 h, and the corresponding IR spectra of adsorbed CO are presented in Fig. 10. A characteristic band at 2103 cm^{-1} is observed for MoP/SiO_2, suggesting a full sulfidation of the surface of MoP/SiO_2 (Fig. 10a). Three IR bands are observed for CO adsorbed on sulfided Ni_2P/SiO_2 catalysts (Fig. 10e). A shift from 2082 cm^{-1} for CO adsorption on the reduced Ni_2P/SiO_2 catalyst to a higher wavenumber at 2094 cm^{-1} with a dramatic decrease in intensity for CO adsorption on the Ni_2P/SiO_2 catalyst pretreated in a H_2S/H_2 mixture is due to the sulfidation of the catalyst. The band at 2094 cm^{-1} is assigned to CO terminally bonded to Ni sites, the band at 2056 cm^{-1} is assigned to the formation of $Ni(CO)_4$, and the band at 2198 cm^{-1} is ascribed to the formation of surface-bonded P=C=O species [33].

Three characteristic bands are obtained for Ni–Mo–P/SiO_2 (Ni/Mo = 0.3, 1.0, and 1.9) after sulfidation in a flowing H_2S/H_2 mixture, i.e., 2102 and 2092 cm^{-1} for a Ni/Mo molar ratio of 0.3 (Fig. 10b), 2103 and 2093 cm^{-1} for a Ni/Mo molar ratio of 1.0 (Fig. 10c), and 2104 and 2093 cm^{-1} for a Ni/Mo molar ratio of 1.9 (Fig. 10d). The IR bands at higher frequencies (2102, 2103, and 2104 cm^{-1}) can be due to CO adsorbed on sulfided Mo sites and the bands at 2092, 2093 can be ascribed to CO adsorbed on sulfided Ni sites on the surface of Ni–Mo–P/SiO_2 samples [25,

33]. It is apparent that H_2S/H_2 can sulfide the surface of phosphide catalysts much easier than thiophene/H_2.

4. Discussion

4.1. BET surface area, TEM, and CO chemisorption

The S_{BET} values of MoP/SiO_2, Ni_2P/SiO_2, and Ni–Mo–P/SiO_2 are lower than that of the silica support (Table 1). For the Ni–Mo–P/SiO_2 catalysts with different Mo and Ni loadings, the S_{BET} values did not change much. Since Ni_2P/SiO_2 has the highest DBT HDS activity but the lowest S_{BET} value (Figs. 3 and 4), the results reveal that the S_{BET} value has no apparent influence on the DBT HDS reaction. MoP/SiO_2 and Ni_2P/SiO_2 have larger pore diameters. The pore diameter decreases when Ni–Mo is supported on the surface of the silica, but it seems that there is no apparent effect of the pore diameter on the catalytic behavior for these phosphide catalysts. This is reasonable since the pore diameters of all catalysts are much larger than the sizes of the reactants and products. It is possible that most Mo and Ni metals are located on the outer surface and not in the inner pores of the silica support.

The TEM morphology of MoP/SiO_2 reveals that the MoP particles have an average particle size around 3 nm (Fig. 2a). A clustering of small particles is observed and the average particle size increases to around 5 nm for Ni_2P (Fig. 2b). This agrees with the absence of XRD peaks for the Ni_2P/SiO_2 catalyst with 15 wt% NiO, suggesting that the crystallites are smaller than 5 nm. Ni–Mo–P shows an average particle size of 4 nm (Fig. 2c), between the particle sizes of MoP and Ni_2P. It is possible that the particle size of pure NiMoP is smaller than that of pure Ni_2P. This is consistent with the order of the S_{BET} values for these phosphide catalysts. These average particle sizes are all somewhat smaller than those reported in the literature [17,27]. The groups of Oyama and Prins reported crystallite sizes of 15 nm in 8.3–13 wt% MoP/SiO_2 catalysts. The crystallite size of Ni_2P/SiO_2 is also smaller than the sizes reported by Wang et al. [18] and Stinner et al. [1] of 20 and 45 nm, respectively, with Ni_2P loadings less than 10 wt%. Rodriguez et al. [24] reported that the mean crystallite sizes of MoP/SiO_2 (25 wt%), Ni_2P/SiO_2 (30 wt%), and $NiMoP/SiO_2$ (NiMoP, 30 wt%) are 13, 28, and 8 nm, respectively.

It should be noted that there is an inverse trend between the CO chemisorption capacity and the DBT HDS activity for MoP/SiO_2, Ni–Mo–P/SiO_2, and Ni_2P/SiO_2 catalysts (Table 2). The MoP/SiO_2 catalyst has the highest CO chemisorption capacity, but the lowest DBT HDS activity. The Ni_2P/SiO_2 catalyst has the lowest CO chemisorption capacity, but its DBT HDS activity and its TOF value are significantly higher than those of the MoP/SiO_2 and Ni–Mo–P/SiO_2 catalysts. The CO chemisorption capacity of Ni–Mo–P/SiO_2 decreases with the addition of Ni, while the HDS activity and TOF value increase. We do not know how CO chemisorbs on to the catalyst, but it is likely that it interacts with exposed metal atoms, not blocked by phosphorous [37]. Similar results were reported by Oyama [2], who found that Ni_2P had a substantially higher activity than MoP in the HDS reaction, but that the values of CO chemisorption for Ni_2P/SiO_2 (10 wt%) and MoP/SiO_2 (13 wt%) were 28 and 50 μmol/g, respectively. Recently, oxygen (O_2) pulsed chemisorption and thiophene HDS activity measurement on phosphided Mo, Ni, and NiMo supported on silica catalysts have been reported by Rodriguez et al. [24]. This research results indicated that although 30 wt% $NiMoP/SiO_2$ exhibited a higher O_2 chemisorption capacity (184.6 μmol O_2/g) than 30 wt% Ni_2P/SiO_2 (166.1) and 25 wt% MoP/SiO_2 (119.6), the HDS activity of $NiMoP/SiO_2$ was much lower than that of Ni_2P/SiO_2 and MoP/SiO_2. These results mean that CO chemisorption cannot be used to compare the HDS activity of different metal phosphides.

4.2. Catalytic performance of silica-supported MoP, Ni_2P, and Ni–Mo–P catalysts

The HDS activity measurements indicate a great difference in the DBT HDS activity of the Ni_2P/SiO_2, MoP/SiO_2, and Ni–Mo–P/SiO_2 catalysts. The TOF value of Ni_2P/SiO_2 is 50 times higher than that of MoP/SiO_2 if the stoichiometry of a CO/active site is assumed to be 1. The IR results show that there is a small peak at 1912 cm^{-1} for CO adsorption on reduced Ni_2P/SiO_2 in Fig. 7e, indicative of CO adsorption on Ni bridge sites, for which there is one CO per two Ni sites. In addition, the asymmetry of the CO absorbance feature at 2082 cm^{-1} suggests a small amount of $Ni(CO)_4$ formation for which an absorbance is observed at 2056 cm^{-1}. Thus, the TOF values for these phosphides are only estimates since there is more than one active site in phosphides. However, the TOF value of Ni_2P/SiO_2 must be higher than that of MoP/SiO_2 and Ni–Mo–P/SiO_2. The Ni_2P/SiO_2 catalyst gives the highest BP and CHB yields, while the MoP/SiO_2 catalyst shows the lowest BP yield owing to its low conversion (cf. Figs. 4–6 and Table 3). Therefore, the order of the HDS activities of DBT on MoP/SiO_2, Ni_2P/SiO_2, and Ni–Mo–P/SiO_2 catalysts is: Ni_2P/SiO_2 > Ni–Mo–P/SiO_2 > MoP/SiO_2. Moreover, Ni_2P/SiO_2 has an eight times higher conversion and a six times higher BP yield than MoP/SiO_2. These results are consistent with those published by Oyama et al. [20] and Sawhill et al. [22], in which a Ni_2P/SiO_2 catalyst was substantially more active for thiophene HDS than sulfided Ni/SiO_2, Mo/SiO_2, and Ni–Mo/SiO_2 (Ni/Mo = 0.5) catalysts, even more active than a commercial sulfided Co–Mo/Al_2O_3 catalyst (Ketjen fine 756). Also Zuzaniuk and Prins concluded that NiMoP and CoMoP catalysts are less active than Ni_2P, Co_2P, and MoP catalyst, from HDN and not HDS [27]. In this study, the main product of DBT HDS is BP for these phosphide catalysts.

The activity results show that metal Ni is not a promoter and should be regarded as the main active component in Ni–Mo–P/SiO_2 catalysts. The DBT HDS data and the IR

spectroscopic data for CO adsorption on the reduced Ni–Mo–P/SiO_2 and reduced mechanically mixed MoP/SiO_2 and Ni_2P/SiO_2 catalysts suggest that the activity of the Ni–Mo–P catalysts is controlled by the available Ni sites and that there are similar active sites on these phosphide catalysts. It is possible that pretreatment (i.e., reduction at 873 K) of the mechanically mixed catalysts converts the phosphide phases to structures similar to those present in the Ni–Mo–P/SiO_2 catalysts. This results in their similar DBT HDS activities. The DBT conversions increase with increasing Ni content for these phosphide catalysts. No synergetic effect of Ni and Mo in Ni–Mo–P/SiO_2 catalysts was observed. This behavior of the phosphides is different from those of the sulfides, carbides, and nitrides reported in the literature [38–40]. For the latter, Ni and Co are the effective promoters that enhance and maintain the catalytic performance of Mo or W. In contrast, there is no synergetic effect in phosphides in the HDS reaction. Moreover, the fact that the HDS activity of Ni_2P/SiO_2 is substantially higher than that of MoP/SiO_2 suggests that the HDS reaction mainly occurs on Ni sites in the Ni–Mo–P/SiO_2 catalyst. This is perhaps one of the unique properties of phosphide catalysts, different from the sulfide, carbide, and nitride catalysts.

4.3. The surface sites and evolution of the surface sites under sulfiding conditions of MoP/SiO_2, Ni_2P/SiO_2, and Ni–Mo–P/SiO_2 catalysts

A characteristic band at 2042 cm^{-1} is observed for CO adsorbed on reduced MoP/SiO_2 (Fig. 7a), which can be attributed to linearly bonded CO on the cus $Mo^{\delta+}$ ($0 < \delta \leqslant 2$) sites on the surface of the reduced MoP/SiO_2 sample [25]. Three distinct CO absorbance bands are observed in the IR spectra of CO adsorbed on reduced Ni_2P/SiO_2 catalysts due to

(1) CO adsorption atop Ni sites,
(2) CO adsorption on Ni bridge sites, and
(3) formation of adsorbed $Ni(CO)_4$ (Fig. 7e).

The band at 2082 cm^{-1} can be due to CO linearly adsorbed on cus $Ni^{\delta+}$ ($0 < \delta < 1$) sites of the reduced Ni_2P/SiO_2 catalyst. This is similar to the result reported by Layman and Bussell [33] except that no absorbance feature is observed at 2193–2204 cm^{-1} for CO adsorption on reduced Ni_2P/SiO_2, which was assigned to the antisymmetric vibration of a coordinated P=C=O species on the catalyst surface. It may be that the surface of the reduced Ni_2P/SiO_2 catalyst is deficient in P (and possibly that of the MoP/SiO_2 and Ni–Mo–P/SiO_2 catalysts as well) since Oyama and co-workers have shown that TPR of Ni_2P/SiO_2 catalysts above 700 K results in loss of P as gaseous PH_3 [18,37]. For the Ni_2P/SiO_2 catalyst, the frequency and intensity of the CO absorbance associated with the formation of surface-bonded P=C=O species also depend on the reduction conditions [33]. It may be that under the higher reduction temperature (i.e., 873 K), some surface P that would otherwise form P=C=O species is hydrogenated and volatilized as PH_3. When Ni_2P/SiO_2 was pretreated with a flowing 10 mol% H_2S/H_2 mixture at 593 K for 1 h, a very weak band at 2198 cm^{-1} due to the formation of P=C=O species is observed (Fig. 10e).

For the Ni–Mo–P/SiO_2 catalysts with a Ni/Mo molar ratio of 1.0, the IR spectrum of adsorbed CO only shows a single band at 2086 cm^{-1} (Fig. 7c), which is ascribed to CO adsorbed on Ni sites. No characteristic band of CO adsorbed on Mo sites is observed. For the NiMoP/SiO_2, it is possible that much of the metallic Ni is exposed on the outer surface of the catalyst because of favored crystallographic orientations or segregation of Ni to the surface. This would make the catalyst surface similar to that of Ni_2P/SiO_2. That is consistent with the HDS results that the DBT conversion of Ni–Mo–P/SiO_2 catalysts increases with increasing Ni content (Fig. 4). It is also identical to the pulsed CO chemisorption results, in which the chemisorption capacity of Ni–Mo–P/SiO_2 decreases with increasing Ni content and which results in a chemisorption capacity of Ni–Mo–P/SiO_2 (Ni/Mo = 1.9) close to that of Ni_2P/SiO_2.

Although metal phosphides are considered to have metallic properties [41], CO adsorption indicates that the Mo and Ni atoms in phosphides are positively charged due to the charge transfer from Mo and Ni to the electronegative P atoms. The XPS study of molybdenum phosphides showed a binding energy of 228.4 eV for phosphided Mo [22]. Considering the electron transfer from Mo to P in MoP and MoP/SiO_2, the authors assigned this binding energy to a $Mo^{\delta+}$ ($0 < \delta \leqslant 4$) species. The XPS analysis of unsupported Ni_2P and Ni_2P/SiO_2 catalysts also indicated a slight transfer of electron density from Ni to P [23].

The IR results in Fig. 7 show that CO is strongly and reversibly adsorbed on the reduced MoP/SiO_2, Ni_2P/SiO_2, and Ni–Mo–P/SiO_2 catalysts. This is different from CO on fully reduced Mo and Ni catalysts on which most CO is dissociatively adsorbed and the remaining CO molecules are weakly bonded and can be removed by prolonged evacuation at room temperature [28–30]. The adsorption behavior of CO on the surface Mo and Ni atoms of reduced MoP and Ni_2P is greatly modified by the presence of P atoms, which distinguishes the surface properties of metallic phosphides from those of metallic nitrides [31,32] and carbides [42]. Layman and Bussell indicated that the P species in the Ni_2P/SiO_2 catalyst increased the dispersion of Ni on the silica support [33].

Our previous work indicated that the passivation layer on MoP/SiO_2 could be completely removed by H_2 above 873 K. Even when the reduction temperature is higher than 723 K, Mo sites on MoP/SiO_2 catalyst are activated to a low valence state [25]. A recent time-resolved XRD study on the preparation of MoP and MoP/SiO_2 from oxide precursors suggested that the reduction of phosphate-type species (PO_x) is the final and determining step in the formation of MoP [24]. The ^{31}P MAS NMR results of MoP/SiO_2 also indicated that surface phosphate species are formed upon passivation of a

fresh MoP/SiO_2 sample and can be removed by a H_2 reduction at 673 K [27]. Considering the preparation temperature for Ni_2P/SiO_2 and Ni–Mo–P/SiO_2, it is possible that oxygen atoms in the passivation layer of these phosphide catalysts can be completely removed or that Mo and Ni sites are activated to a low valence state by H_2 treatment at temperatures above 873 K. Therefore, the differences in the surface states could be one of the reasons that phosphides exhibit better catalytic activities in hydrotreating reactions than the corresponding nitride and carbide catalysts, whose working surfaces are actually in a oxynitride or oxycarbide form after H_2 activation [10,32]. The DBT HDS activity results reveal that phosphide catalysts show an unusual trend of stable or increasing activity over reaction time in the initial stage of the reaction. This behavior was first reported by Bussell and coworkers for different phosphides in thiophene HDS [22–24]. This unique catalytic performance of phosphides also distinguishes them from nitrides and carbides. Mo_2N and Mo_2C catalysts either showed a decreased activity during the whole HDS reaction or a stable activity after a decrease in the initial reaction stage [10,43].

The nature of the surface sites of these phosphides under DBT HDS reaction can be well correlated to the IR investigation in which the samples are pretreated by a mixture of thiophene/H_2 or H_2S/H_2 under conditions similar to those in the DBT HDS reactivity tests. When the MoP/SiO_2 sample is pretreated with thiophene/H_2, a new band at 2089 cm^{-1} appears which can be assigned to adsorbed CO on sulfided Mo sites (Fig. 9a), suggesting that the surface of the MoP/SiO_2 catalyst became partially sulfided. This is consistent with the results reported by Wu et al. [25]. The authors also found that the sulfided MoP/SiO_2 could be fully reactivated to a fresh phosphide catalyst under mild conditions. The structure of MoP may persist while the phosphide surface is modified by sulfur under HDS conditions.

The characteristic IR band at 2082 cm^{-1} attributed to adsorbed CO on reduced Ni_2P/SiO_2 shifts to 2080 cm^{-1} when Ni_2P/SiO_2 is pretreated with a mixture of thiophene/H_2, and the intensity decreases (Fig. 9e). It is likely that the surface of Ni_2P/SiO_2 has not been sulfided under this sulfidation condition since no upward shift in frequency is observed. The decrease in the CO absorbance, assigned to CO terminally bonded to Ni sites, indicates a decrease in the number of these sites available for CO adsorption. The treatment of the phosphide catalysts in thiophene/H_2 mixtures may have led to deposition or incorporation of S and C on the surface of the catalysts. As a result, some of the sites are blocked and not available for CO adsorption. It is possible that Mo is more easily sulfided under the same sulfidation conditions than Ni in phosphides, as described in Fig. 9.

The characteristic IR band at 2082 cm^{-1} for adsorbed CO on reduced Ni_2P/SiO_2 shifts to 2094 cm^{-1} for Ni_2P/SiO_2 pretreated with H_2S/H_2 with a large decrease in intensity (Fig. 10e). It indicates that the surface of Ni_2P/SiO_2 has been partially sulfided. The upward shift in frequency and significant decrease in intensity show that S deposits on the surface of Ni_2P/SiO_2, blocking some of the sites available for CO adsorption and withdrawing electron density from Ni sites. P atoms may also serve as sites for the adsorption and bonding of S-containing species. It is probable that a phosphosulfide layer is formed on top of the surface of Ni_2P/SiO_2, in accordance with results reported by Oyama and co-workers [2,21,37]. The authors observed the formation of Ni–S linkages at the surface of the supported Ni_2P particles by elemental analysis and EXAFS measurements of catalysts tested under HDS conditions. They also found that the XRD peak positions for the spent samples after 100 h on stream did not change, demonstrating that the Ni_2P was stable under the hydrotreating conditions. From in situ XAFS studies, Kawai et al. concluded that the Ni_2P structure was stable under reaction conditions and was an active structure for the HDS process [44]. Zuzaniuk and Prins suggested that physisorbed H_2S could be present both on the support and on the metal phosphide particles and that surface sulfidation of the metal phosphides may also have taken place [27]. Korányi [45] and Robinson et al. [46] reported that $NiPS_3$ decomposed to Ni_2P, even in the presence of H_2S. Layman and Bussell recently reported that a passivated Ni_2P/SiO_2 catalyst subjected to a sulfidation pretreatment had a higher thiophene HDS activity than a sample of the same catalyst subjected to reduction pretreatment [33]. Combined with our IR spectra results, we conclude that the surface of these phosphides can be partially sulfided and a phosphosulfide phase is formed on the surface of the catalyst under HDS conditions, and that the active Ni_2P/SiO_2 catalyst in HDS reaction is probably a NiP_xS_y phase in the outer region of the Ni_2P crystallite.

It seems that Ni functions as a promoter in the sulfidation of Mo on the surface of the Ni–Mo–P/SiO_2 sample, as with increasing Ni/Mo molar ratio the extent of molybdenum sulfiding is higher (Fig. 9b, 9c, and 9d). The IR results indicate that the catalysts are actually partially sulfided after 6 h on stream. The surfaces of the phosphide catalysts evolve into a more active form with time on stream. Meanwhile, the structure of the phosphides can be retained under HDS reactions. The evolved surface sites also show some differences from those of sulfided Mo or sulfided Ni in our IR studies [25,33]. This unique surface constitution of NiP_xS_y is probably responsible for the high catalytic activity of Ni_2P/SiO_2 catalyst in DBT HDS. This again suggests that phosphides are potential substitutes for conventional sulfide catalysts in hydrotreating processes; especially nickel phosphide is a more promising novel catalytic material owing to its unique intrinsic high catalytic activity.

4.4. HDS mechanism of dibenzothiophene

Fig. 11 gives the mechanism of the HDS of DBT. The DBT reaction products are biphenyl, cyclohexylbenzene, and traces of tetrahydrodibenzothiophene. The transformation of DBT occurs through two paralled reactions, namely, (i) direct desulfurization (DDS) yielding BP and then BP hy-

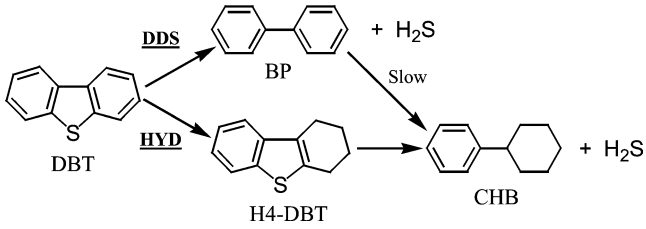

Fig. 11. Mechanism of the HDS of dibenzothiophene (DBT) on phosphide catalysts. The products are biphenyl (BP), cyclohexylbenzene (CHB), and tetrahydrodibenzothiophene (H4-DBT).

drogenation yielding CHB, and (ii) desulfurization after hydrogenation (HYD), first yielding H4-DBT and then CHB. From the DBT HDS activities, it is clear that BP produced by the DDS route is the main product with a selectivity higher than 65%. CHB can be produced by BP hydrogenation or by H4-DBT desulfurization. The intermediate product H4-DBT has the lowest selectivity, less than 10%. DBT is mainly desulfurized by the DDS route over phosphide catalysts, because BP instead of CHB is obtained as the major product. This is very similar to the results obtained for sulfide catalysts [47].

5. Conclusions

Silica-supported binary and ternary transition metal phosphides (MoP, Ni_2P, and Ni–Mo–P) have been prepared from inexpensive phosphate precursors by reduction in hydrogen. Their DBT HDS activities are in the order: $Ni_2P/SiO_2 >$ Ni–Mo–$P/SiO_2 >$ MoP/SiO_2. The presence of Ni in the Ni–Mo–P/SiO_2 catalysts has a significant effect on the conversion of DBT and the activity of the catalysts increases with increasing Ni content. This is different from sulfides, nitrides, and carbides, as no synergetic effect is observed between phosphided Ni and Mo atoms.

CO adsorbed on reduced MoP/SiO_2 and Ni_2P/SiO_2 catalysts show characteristic IR bands at 2042 and 2082 cm^{-1}, respectively, which are ascribed to CO linearly bonded to cus $Mo^{\delta+}$ ($0 < \delta \leqslant 2$) sites of the reduced MoP/SiO_2 catalyst and $Ni^{\delta+}$ ($0 < \delta < 1$) sites of the reduced Ni_2P/SiO_2 catalyst. The IR results suggest that Ni species are more easily exposed at the surface of the NiMoP particles and that Ni seems to promote the sulfidation of Mo. The IR results also indicate that the surface of these phosphide catalysts is partially sulfided. A surface phosphosulfide phase may be formed while the bulk structure of the phosphides is retained under HDS reaction conditions. This surface nickel phosphosulfide phase (NiP_xS_y) may be responsible for the high and stable activity of the Ni_2P/SiO_2 catalyst.

For MoP/SiO_2, Ni_2P/SiO_2, and Ni–Mo–P/SiO_2 catalysts, the transformation of DBT mainly occurs through direct desulfurization yielding biphenyl. The reactivity and spectroscopic results suggest that nickel phosphide is potentially a promising catalyst for hydrodesulfurization processing.

Acknowledgments

This work was supported by the State Key Project of the Ministry of Science and Technology of China (Grant G 2000048003) and the National Natural Science Foundation of China (NNSFC) (Grant 20303018).

References

[1] C. Stinner, Z. Tang, M. Haouas, T. Weber, R. Prins, J. Catal. 208 (2002) 456.
[2] S.T. Oyama, J. Catal. 216 (2003) 343.
[3] P. Grange, Catal. Rev.-Sci. Eng. 21 (1980) 135.
[4] E. Furimski, Catal. Rev.-Sci. Eng. 22 (1980) 371.
[5] R. Iwamoto, J. Grimblot, Adv. Catal. 44 (1999) 417.
[6] P. Atanasova, A.L. Agudo, Appl. Catal. B 5 (1995) 329.
[7] D.D. Whitehurst, T. Isoda, I. Mochida, Adv. Catal. 42 (1998) 345.
[8] A.J. Wang, Y. Wang, T. Kabe, Y.Y. Chen, A. Ishihara, W.H. Qian, J. Catal. 199 (2001) 19.
[9] S.T. Oyama, C.C. Yu, S. Ramanathan, J. Catal. 184 (1999) 535.
[10] P.A. Aegerter, W.W.C. Quigley, G.J. Simpson, D.D. Ziegler, J.W. Logan, K.R. McCrea, S. Glazier, M.E. Bussell, J. Catal. 164 (1996) 109.
[11] W. Qian, Y. Yoda, Y. Hirai, A. Ishihara, T. Kabe, Appl. Catal. A 184 (1999) 81.
[12] C. Song, K.M. Reddy, Appl. Catal. A 176 (1999) 1.
[13] C. Stinner, R. Prins, T. Weber, J. Catal. 202 (2001) 187.
[14] W. Li, B. Dhandapani, S.T. Oyama, Chem. Lett. (1998) 207.
[15] S.T. Oyama, P. Clark, V.L.S. Teixeira da Silva, E.J. Lede, F.G. Requejo, J. Phys. Chem. B 105 (2001) 4961.
[16] P. Clark, W. Li, S.T. Oyama, J. Catal. 200 (2001) 140.
[17] P. Clark, X. Wang, S.T. Oyama, J. Catal. 207 (2002) 256.
[18] X. Wang, P. Clark, S.T. Oyama, J. Catal. 208 (2002) 321.
[19] S.T. Oyama, P. Clark, X. Wang, T. Shido, Y. Iwasawa, S. Hayashi, J.M. Ramallo-Lopez, F.G. Requejo, J. Phys. Chem. B 106 (2002) 1913.
[20] S.T. Oyama, X. Wang, F.G. Requejo, T. Sato, Y. Yoshimura, J. Catal. 209 (2002) 1.
[21] S.T. Oyama, X. Wang, Y.K. Lee, K. Bando, F.G. Requejo, J. Catal. 210 (2002) 207.
[22] S.J. Sawhill, D.C. Phillips, M.E. Bussell, J. Catal. 215 (2003) 208.
[23] D.C. Phillips, S.J. Sawhill, R. Self, M.E. Bussell, J. Catal. 207 (2002) 266.
[24] J.A. Rodriguez, J.Y. Kim, J.C. Hanson, S.J. Sawhill, M.E. Bussell, J. Phys. Chem. B 107 (2003) 6276.
[25] Z.L. Wu, F.X. Sun, W.C. Wu, Z.C. Feng, C.H. Liang, Z.B. Wei, C. Li, J. Catal. 222 (2004) 41.
[26] JCPDS Powder Diffraction File, International Center for Diffraction Data, Swarthmore, PA, 2000.
[27] V. Zuzaniuk, R. Prins, J. Catal. 219 (2003) 85.
[28] J.B. Peri, J. Phys. Chem. 86 (1982) 1615.
[29] M.L. Colaianni, J.G. Chen, W.H. Weinberg, J.T. Yates Jr., J. Am. Chem. Soc. 114 (1992) 3735.
[30] B. Müller, A.D. van Langeveld, J.A. Moulijn, H. Knözinger, J. Phys. Chem. 97 (1993) 9028.
[31] S.W. Yang, C. Li, J. Xu, Q. Xin, J. Chem. Soc., Chem. Commun. 13 (1997) 1247.
[32] S.W. Yang, C. Li, J. Xu, Q. Xin, J. Phys. Chem. 102 (1998) 6986.
[33] K.A. Layman, M.E. Bussell, J. Phys. Chem. B 108 (2004) 10,930.
[34] L.H. Little (Ed.), Infrared Spectra of Adsorbed Species, Academic Press, London, 1966.
[35] J.T. Yates Jr., C.W. Garland, J. Phys. Chem. 65 (1961) 617.
[36] L. Kubelková, J. Nováková, N.I. Jaeger, G. Schulz-Ekloff, Appl. Catal. A 95 (1993) 87.
[37] S.T. Oyama, X. Wang, Y.K. Lee, W.J. Chun, J. Catal. 221 (2004) 263.
[38] D.D. Whitehurst, T. Isoda, I. Mochida, Adv. Catal. 42 (1998) 345.
[39] J. Mijoin, V. Thévenin, N.G. Agurre, H. Yuze, J. Wang, W.Z. Li, G. Pérot, J.L. Lemberton, Appl. Catal. A 180 (1999) 95.

[40] Y.J. Chu, Z.B. Wei, S.W. Yang, C. Li, Q. Xin, E.Z. Min, Appl. Catal. A 176 (1999) 17.
[41] B. Aronsson, T. Lundström, S. Rundqvist, Borides, Silicides, and Phosphides, Methuen/Wiley, London, 1965.
[42] W.C. Wu, Z.L. Wu, C.H. Liang, X.W. Chen, P.L. Ying, C. Li, J. Phys. Chem. B 107 (2003) 7088.
[43] K.R. McCron, J.W. Logan, T.L. Tarbuck, J.L. Heiser, M.E. Bussell, J. Catal. 17 (1997) 255.
[44] T. Kawai, S. Sato, S. Suzuki, W.J. Chun, K. Asakura, K.K. Bando, T. Matsui, Y. Yoshimura, Y. Okamoto, Y.K. Lee, S.T. Oyama, Chem. Lett. 32 (2003) 956.
[45] T.I. Korányi, Appl. Catal. A 239 (2003) 253.
[46] W.R.A.M. Robinson, J.N.M. van Gestel, T.I. Korányi, S. Eijsbouts, A.M. van der Kraan, J.A.R. van Veen, V.H.J. de Beer, J. Catal. 161 (1996) 539.
[47] M. Egorova, R. Prins, J. Catal. 224 (2004) 278.